



UNIVERSIDAD DEL ISTMO

www.unistmo.edu.mx

"2020, AÑO DE LA PLURICULTURALIDAD DE LOS PUEBLOS INDÍGENAS Y AFROMEXICANO"

OFICIO No. 066/DGA/UNISTMO/2020

Asunto: *Gastos De publicación, Solicitud de Liberación.*
Sto. Domingo Tehuantepec, Oax., 19 de noviembre de 2020

Lic. Lorenzo Manuel Loera de la Rosa
Director de Superación Académica

ATN:

Lic. Graciela Hernández Sánchez

Subdirectora de Análisis y Evaluación Docente

Por este conducto le envío un cordial saludo, al tiempo que remito la **Solicitud de Liberación** correspondiente al *apoyo para Gastos de Publicación* autorizado al **PTC FRANCISCO AGUILAR ACEVEDO**, adscrito a la Universidad del Istmo. Cabe señalar que el apoyo fue autorizado mediante oficio No. 511-6/2020-6390, de fecha 23 de marzo de 2020.

<i>Nombre del PTC</i>	<i>Revista / ISSN</i>	<i>Título del artículo</i>	<i>Costo (M.N.)</i>
<i>M. C. Francisco Aguilar Acevedo</i>	Fractals / 0218-348X	ROBOTIC ARM WITH BIOT MACHINE LEARNING SYSTEM	\$25,000.00

Se adjunta solicitud de liberación por parte del PTC en comento, Informe final (impacto académico logrado), copia del artículo publicado; y desglose financiero de recursos que emite la Universidad del Istmo. Los documentos en PDF se enviaron al correo victorh.osornio@nube.sep.gob.mx.

Garantizando la transparencia en el ejercicio de los recursos, agradezco la atención prestada al presente, y aprovecho la ocasión para agradecer los apoyos que nos brinda el Programa en mejora de la educación de nuestra región, nuestro estado y por ende nuestro país.

A T E N T A M E N T E

*Voluntas totum potest
Guiraa zanda ne gandaracala 'dxi'*

L.C.E. Claudia Hernández Cela
Jefa del Departamento de Gestión Académica

C.f.p. -Dr. Modesto Seara Vázquez.- Rector de la Universidad del Istmo.- Para su conocimiento.
-Dr. Israel Flores Sandoval.- Vice-rector Académico.- Universidad del Istmo.- Mismo fin.
-M.C. Francisco Aguilar Acevedo.- Profesor-Investigador.- Universidad del Istmo.- para seguimiento.
- Archivo

*CHC/

Campus Tehuantepec
Cd. Universitaria, Sto. Domingo
Tehuantepec, Oax.
(971) 5224050

Campus Ixtepec
Cd. Universitaria, Cd. Ixtepec, Oax.
(971) 7127050

Campus Juchitán
Cd. Universitaria, H. Cd. de Juchitán de
Zaragoza, Oax.
(971) 712 7050

Sto. Domingo Tehuantepec Oaxaca a 15 de octubre de 2020

Asunto: Gastos de publicación,
Solicitud de Carta de Liberación.

Lic. Lorenzo Manuel Loera de la Rosa
Director de Superación Académica

AT'N: Lic. Graciela Hernández Sánchez
Subdirectora de Análisis y Evaluación Docente

Sirva el presente para enviarle un cordial saludo y mi agradecimiento por el apoyo recibido en el proyecto Gastos de Publicación. Así mismo, aprovecho la ocasión para solicitarle de la manera más respetuosa la **Carta de Liberación** correspondiente al apoyo recibido en mérito del Programa, autorizado en el oficio No. 511-6/2020-6390 de fecha 03 de septiembre de 2020. Es importante comentar que el artículo titulado "ROBOTIC ARM WITH IoT MACHINE LEARNING SYSTEM", se publicó en la revista Fractals, con ISSN (impreso) 0218-348X, ISSN (en línea) 1793-6543, en el volumen 28 número 4, de fecha 12 de mayo de 2020.

Se adjunta al presente, copia del artículo publicado en revista indexada, así como, informe final que contiene el impacto académico logrado con el apoyo recibido.

Sin más por el momento quedo de usted.

ATENTAMENTE.

"Voluntas totum potest"
Guirá' zanda ne quend'racala'dxi'



M.C. Francisco Aguilar Acevedo
Profesor-Investigador

C.c.p. -Dr. Israel Flores Sandoval.- Vice-rector Académico.- Universidad del Istmo.-Para su conocimiento.
.-L.C.E. Claudia Hernández Cela.- Representante Institucional ante el Programa.- Universidad del Istmo.-Mismo fin.
.-Archivo



Universidad del Istmo

INFORME FINAL

GASTOS DE PUBLICACIÓN

IES de adscripción:	Universidad del Istmo	Título de la publicación:	ROBOTIC ARM WITH BIOT MACHINE LEARNING SYSTEM
Nombre del PTC:	Francisco Aguilar Acevedo	Nombre de la Revista:	FRACTALS
ID del PTC:	111329	ISSN:	0218-348X
Número de oficio de autorización:	511-6/2020-6390	Link: (opcional)	https://doi.org/10.1142/S0218348X20500887
Fecha de autorización:	03 de septiembre de 2020	Monto aprobado	\$25,000.00

Impacto académico logrado con el apoyo recibido:

El artículo publicado hasta el momento del presente informe ha tenido 101 descargas.


M.C. Francisco Aguilar Acevedo
Profesor-Investigador


L.C.E. Claudia Hernández Cela
Representante Institucional ante
PRODEP



UNIVERSIDAD DEL ISTMO



PROGRAMA PARA EL DESARROLLO PROFESIONAL DOCENTE, PARA EL TIPO SUPERIOR 2020

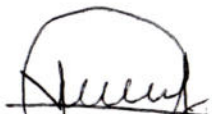
OFICIO APROBACION DSA 511-6/2020-6390 03'SEPT'2020

GASTOS DE PUBLICACIÓN

Beneficiario : FRANCISCO AGUILAR ACEVEDO

Fecha	No. Ch. / T.E.	No. Comprobante	Beneficiario del Pago	R.F.C.	Concepto del Gasto	IMPORTE FACTURA (Ejercido)	GASTOS DE PUBLICACIÓN
Monto Aprobado						\$	25,000.00
22/10/2020	305119	001/511-6/2020-6390	REVISTA " FRACTALS" DOI: S0218348X20500887	***	PAGO DE PUBLICACIÓN DEL ARTICULO " ROBOTIC ARM WITH BIOT MACHINE LEARNING SYSTE"	\$ 25,000.00	\$ -
Total Gastos						\$	25,000.00

Cd. Ixtepec, Oax. a 4 de Noviembre 2020


L.C. Yazmin Carolina López Morales
 Jefa del Departamento de Recursos Financieros




L.C.E Eugenio Cortés Hernández
 Vice-Rector de Administración



ROBOTIC ARM WITH BIOT MACHINE LEARNING SYSTEM

R. CARREÑO AGUILERA* and F. AGUILAR ACEVEDO
*Universidad del Istmo, Cd. Universitaria S/N, 70760
Tehuantepec, Oaxaca, México*
**ricardo.carreno.a@hotmail.com*

M. PATIÑO ORTIZ and J. PATIÑO ORTIZ
*Instituto Politécnico Nacional
SEPI-ESIME Zacatenco, 07738 México City, México*

Received February 20, 2020

Accepted March 13, 2020

Published May 12, 2020

Abstract

In this work, we present a robotic arm assisted by a visual system to decide whether an object with different colors, parallel flat surfaces and other types of surfaces would be subject to be manipulated without a drop risk. This robotic arm is assisted with sensors such as temperature, humidity, artificial vision, etc. and monitored with a Blockchain Internet of Things (BIoT) expert system assistance, which is shared and accessed by the internet by the users. A prototype for industrial purpose is launched to start providing data for training the expert system, achieving in this way an expert system with machine learning. The variations derived from the identification of the reference points and the characteristics of the robotic arm are a limiting factor of the system, however, it was possible to correctly locate the robotic arm in the workspace to take the object and manipulate it using machine learning based on a BIoT expert system.

Keywords: Machine Learning; Pattern Recognition and BIoT (Blockchain Internet of Things), Vision Control.

*Corresponding author.

This is an Open Access article published by World Scientific Publishing Company. It is distributed under the terms of the Creative Commons Attribution 4.0 (CC-BY) License. Further distribution of this work is permitted, provided the original work is properly cited.

1. INTRODUCTION

Computer vision seeks to help machines to have the ability to perceive and understand an image, to imitate the process that humans perform with their eyes but the integration with blockchain^{1–10} and the internet of things (IoT)^{11–13} now is a need. One of the applications of these systems is recognition, which can be used in areas such as industry, medicine and robotics.¹⁴ The visual control of robots refers to the use of visual information to control the position and/or orientation of a robotic arm to perform a task. Therefore, it is necessary to extract information from an image, which is used to generate the movement of the robotic arm, using kinematic models and control sequences. Although there are works under the theme of visual control of robots, these developments involve the use of industrial-type robots, which coupled with the confidentiality of information, hinders the task of reproducing these systems for educational purposes.

Concerning the recognition of objects, a problem that regularly occurs is the number of sensors needed to acquire useful information. Being there, where the use of image sensors represents an alternative, allowing to obtain more information from the environment looking for more efficient recognition tasks. To do this, there are different types of devices used in visual control¹⁵ where web cameras^{16,17} are used, which uses stereoscopic vision. In this work, the Kinect device is used, which provides information in 2D and 3D through its color camera, an infrared sensor, and a depth sensor.

The visual control of robots is defined as the use of visual information from one or more video cameras, whether fixed or mobile, to control the position and/or orientation of the end effector of a robot concerning an object or a set of visual characteristics of this, depending on the task to be carried out.^{18–22}

The visual control of robots is divided into two main categories: open-loop control also called look-then-move, and visual servo-visual control servoing²³ where the vision system provides inputs to a feedback controller to internally stabilize the robot.²⁴ In the case of open-loop systems, the extraction of image information and the control of the robot are two separate tasks, when first performing the processing and interpretation of the images followed by the generation of a control sequence. In this type of visual control, the robot can execute the task by performing movements that

assume that the environment remains static after the robot has begun to move.

The open-loop control has been approached from different methods. It has developed systems to carry out operations of recognition and manipulation of flexible objects that change their shape during the execution of an action, and where the planning of fixed trajectories often is not applicable.²⁵ The prototype obtains the 3D information of the object and in the background captures through the Kinect the deformation that presents the object when being taken by a Universal Robots Arm UR5 of six degrees of freedom. Also, systems have been developed to identify and collect PVC-type connectors with a Cosero²⁶ robot. The detection of objects in the scene is done by coinciding probabilistic graphics, while for the identification of the geometry of the objects (planes, cylinders, and spheres), the Schnabel algorithm was used, however, this algorithm is found to require artificial intelligence to scale to an industrial massive adoption such that this specific development can be used for general purpose since an expert system^{27–32} using machine learning with deep belief networks as the inference engine^{33,34} can be learning each case of use as long as it is a manipulation use arm robot case; the expert system will be learning the manipulation of very different kinds of geometrical objects with very different types of surfaces but also an IoT platform is required to scale to an industrial level since an arm robot contains a bunch of sensors working together to get the manipulation such that data from this sensors need to be stored in a data base conforming a big data on the cloud from the web to feed the machine learning process, a user may be concern about their data process but they are protected by his blockchain account and only general or common data are shared online. There is also research about the interactive transfer of objects between a human worker and an industrial robot is addressed, using two Kinect to know the location of the object and the human and a planning module that analyzes the current conditions of approach and grip of the robot. In application to the meat industry that has developed the processes of selection and location of pieces of beef, that is a common task in slaughterhouses.^{35,36}

However, robotic arms with artificial vision applications have a big challenge; the variations derived from the identification of the reference points and

the characteristics of the robotic arm are a limiting factor of the system, therefore the main contribution of this research is to make possible to correctly locate the robotic arm in the workspace to take the object and manipulate it using machine learning based on a blockchain internet of things (BIOt) expert system. The expert system is capable to learn to identify the reference points and the specific characteristics of the robotic arm quickly to avoid a big inconvenience with the robotic arm user, this is because the expert system is not only assisted by a deep learning (DL) inference module but also because this inference module can learn faster as the data provided by the sensors is growing as long as it is accumulated in an internet storage (database) with the concept of the IoT. This database is safety thanks to the blockchain developed for this research.

2. METHODOLOGY

Figure 1, the experimental setup for the visual control system is presented. The image processing and interpretation, post-processing, and robot motion planning stages have been made in a high-performance computer. In Fig. 2, the general scheme is shown. The processing and interpretation of the image are done using the resources of the OpenCV free library, obtaining from this stage the lines in 2D candidates to represent edges (common side to two faces) of flat parallel surfaces of the objects (rectangular prisms). Subsequently, correspondence with the 3D data and post-processing is made to define the edges of the flat parallel surfaces and on them identify reference points, which through the kinematic model and a cubic polynomial trajectory are transformed into a movement specification of the Smart Robotic Arm of four

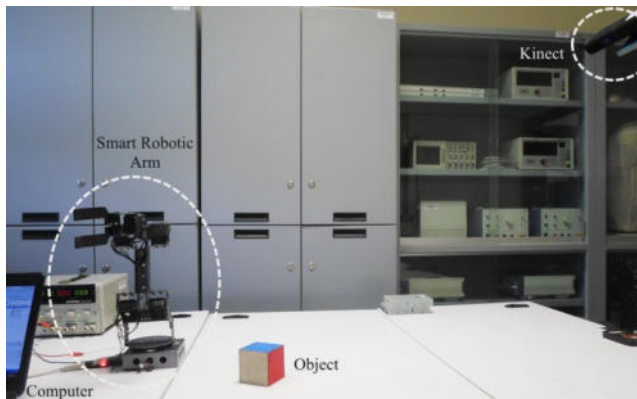


Fig. 1 Experimental setup for visual control system.

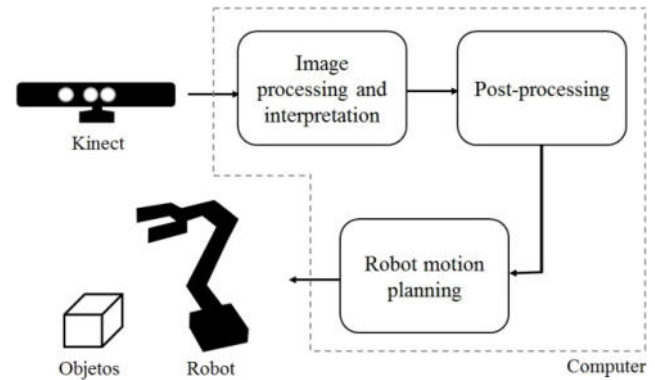


Fig. 2 Visual control for the general scheme.

degrees of freedom. In the following sections, the indicated modules that make up the visual control system proposed are broken down.

3. IMAGE PROCESSING AND INTERPRETATION

This first stage consists in the processing and interpretation of the image data obtained through the Kinect. Figure 3 shows the modules that make up the phases of this stage. The 2D image is generated from the colors associated with the 3D point cloud obtained through the libraries provided by the Kinect SDK. The processing consists of making a crop of the original image to reduce the amount of data to be processed, limiting itself to cover the work area of the manipulator. Then the median filter is used to eliminate noise in the image, and a dilation to reduce the size of the objects and obtain a better correspondence with the depth data. Finally, a Canny filter is applied that allows the detection of edges using two appropriate thresholds (upper and lower) to identify the edges of the objects, under the light conditions in which the tests are carried out.

In the interpretation of the image, the Hough probabilistic transform is used by the Hough Lines P function in OpenCV, which allows detecting lines in a 2D image under certain parameters. Once all the lines in the image have been detected, the pixel value of the initial and final positions of the same in 2D is obtained and correspondence is made with the point cloud to obtain the 3D coordinates. Previously, the 3D data in the reference system of the Kinect, are transformed into the robotic arm system. Therefore, a relationship between the coordinate systems is used, which is shown in Fig. 4, where the robot-Kinect transformation is defined

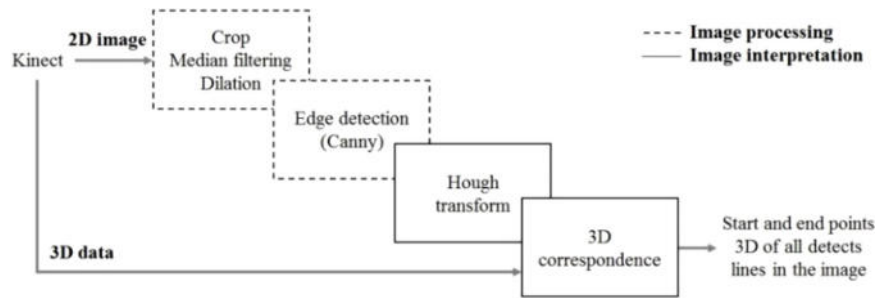


Fig. 3 Image processing and recognition procedure.

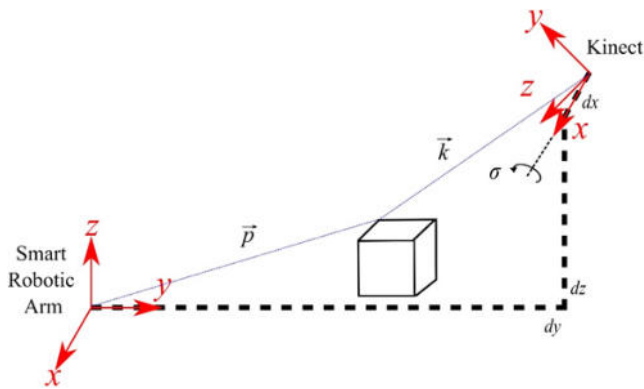


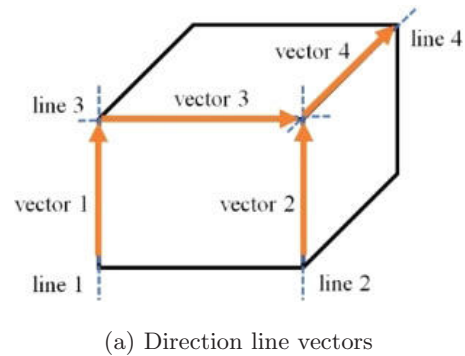
Fig. 4 Coordinate transformation.

as a translation in x , y and z , and rotation over x . Thus, using (1), it is possible to calculate each reference point in the object (p_x, p_y, p_z) with respect to the robot's coordinate system. Being (k_x, k_y, k_z) the point on the object respect to the Kinect coordinate system, and where $\sigma = 137^\circ$, $d_x = 9$ mm, $d_y = 1225$ mm, and $d_z = 800$ mm, for the real test scenario.

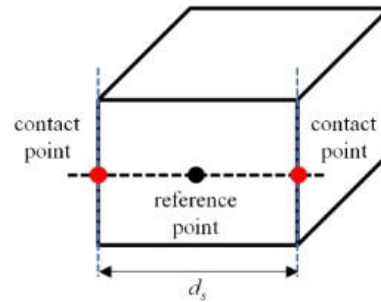
$$\begin{bmatrix} p_x \\ p_y \\ p_z \\ 1 \end{bmatrix} = \begin{bmatrix} 1 & 0 & 0 & d_x \\ 0 & \cos \sigma & -\sin \sigma & d_y \\ 0 & \sin \sigma & \cos \sigma & d_z \\ 0 & 0 & 0 & 1 \end{bmatrix} \begin{bmatrix} k_x \\ k_y \\ k_z \\ 1 \end{bmatrix}. \quad (1)$$

3.1. Post-Processing

An address vector is associated with each detected line (from its starting and ending points), as shown in Fig. 5a. The angle between the vectors of line pairs is obtained from the definition of the point product. If the angle between the vectors is equal to or smaller than ε_1 , parallel lines are considered. The magnitudes of pairs of vectors are compared and if their absolute difference is less than ε_2 , and separation distance d_s is close to the opening size D of the clamp ($D - \varepsilon_3 \leq D \leq D + \varepsilon_4$) they will be



(a) Direction line vectors



(b) Fixing and reference points

Fig. 5 Process for line discrimination.

considered as pairs of lines Parallel valid. This criterion is valid under the slogan that the objects used have the form of rectangular prisms, which implies that their parallel edges are approximately the same size. Once the line discrimination has been done, the midpoint of each line joining two attachment points of the object is obtained (Fig. 5b).

3.2. Robot Motion Planning

The purpose of this module is to transform the reference points into joint values for the motors in the robot, which generate a “soft” movement. Figure 6 shows the modules that make up the planning of the movement.

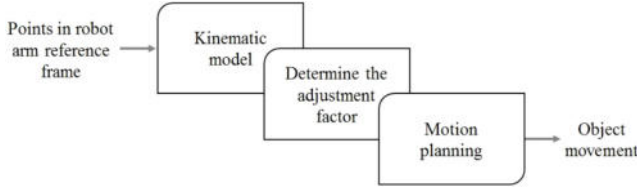


Fig. 6 Movement plan.

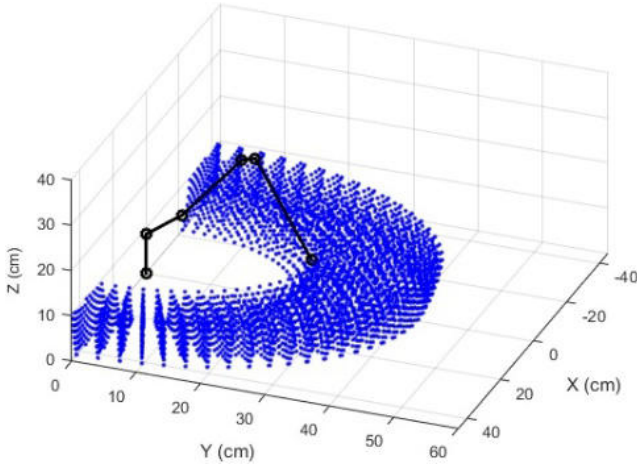


Fig. 7 Isometric view of the restricted workspace of the Smart Robotic Arm.

To define the movement of the robot, it is necessary to establish the direct and inverse kinematic models. The Denavit–Hantenberg convention was used, while the inverse model related to the position was obtained using a geometrical approach.^{37,38,40,41} Figure 7 shows the workspace that is obtained from the direct kinematic model of the Smart Robotic Arm manipulator, and that allowed to estimate the position that the objects must keep in order to be taken by the robot.

Once the angles are obtained for each degree of freedom through the inverse kinematics, it is necessary to adjust the values due to how the motors are anchored to each one of the joints of the robot. Finally, velocity profiles were implemented through a cubic polynomial trajectory (2) for the angular movement of the motors, which allowed for a smooth movement when moving an object from an initial position to an end position, without releasing it. In order to do the description of the cubic polynomial trajectory, it is considered that the robot starts from the idle position.

$$q(t) = q_0 + \frac{3(q_f - q_0)}{t_f^2} t^2 - \frac{2(q_f - q_0)}{t_f^3} t^3. \quad (2)$$

3.3. Motion Stability Study

Defining $M = m \times m$.

Being $M = M^T M = M^T$ a symmetric matrix and if $M = -M^T$ is a non-symmetric matrix, the square matrix is equal to both matrix sum:

$$M = \frac{M + M^T}{2} + \frac{M - M^T}{2}. \quad (3)$$

Considering that a quadratic function $X^T M x$ associated with a non-symmetric matrix is always zero.

$$\begin{aligned} X^T M x &= -X^T M^T x = (-X^T M^T X)^T \\ &= -X^T M x = \emptyset. \end{aligned} \quad (4)$$

Then, $X^T M x$ function with symmetric M is equal to a quadratic function as long as a quadratic matrix ($m \times m$) is defined as positive if

$$\forall X \neq \emptyset \rightarrow X^T M x > \emptyset. \quad (5)$$

The matrix M is defined as positive only if the $X^T M x$ function is defined as positive.

Therefore, a function $\dot{X} = A x$ analyzed with a Lyapunov function $V(X) = X^T M x > \emptyset$ deriving the Lyapunov function we have the following:

$$\begin{aligned} \dot{Y}(X) &= \dot{X}^T M x + X^T M \dot{x} \\ &= X^T A^T M x + X^T M A x, \end{aligned} \quad (6)$$

$$\dot{Y}(X) = X^T A^T M + M A x < \emptyset. \quad (7)$$

$A^T M + M A \rightarrow M$ symmetric.

If the M symmetric matrix are negative, therefore the following inequality:

$$\exists M = M^T > \emptyset : A^T M + M A < \emptyset. \quad (8)$$

In order to solve this, it is possible to transform it to a Lyapunov equation:

$$\begin{aligned} \exists M = M^T > \emptyset, \\ N = N^T > \emptyset : A^T M + M A = -N, \end{aligned} \quad (9)$$

where N is a symmetric matrix defined as positive with $N = I$ (identity).

Let the model considered in state-space have the form (1). In agreement to (1) and, the recursive form is

$$Y_t = G Y_t + H V_t, \quad (10)$$

where G, H are matrices bounded with $G \in \mathbb{R}$ and, $H = f(A, C, B, D), \forall t \in N$.

3.4. Expert System With Machine Learning Used to Identify Parallel Lines on a BIOT System

Once the lines in the image are recognized, it is necessary to determine which are parallel by the post-processing. In this particular case, the experimental parameters of the post-processing are: $\varepsilon_1 = 5^\circ$, $\varepsilon_2 = 30\text{ mm}$, $\varepsilon_3 = 20\text{ mm}$, and $\varepsilon_4 = 10\text{ mm}$. In the case of ε_2 , its value is due to the effect caused by the expansion and application operations of the Hough transform, which caused an unreal increase in the difference in magnitude between parallel lines.

Finally, a test was performed rotating the cube on its axis, to determine the number of parallel lines that was observed in the 2D image and those that the system determined to be parallel from the processing of the 3D data.

Table 1 a maximum of 33.33% recognition of parallel lines was observed when the object is rotated at 0° , 40° and 120° , recognizing two pairs of parallel lines of the six pairs of parallel lines visible in the image. The values where the percentage was zero are due to the error of correspondence between 2D and 3D data (Fig. 8).

In the case of velocity profiles, the times for the movement trajectory (t_f) were defined under two criteria: the maximum amplitude of angular movement ($q_f - q_0$), and the minimization of “abrupt” movements.

In the case of this last criterion, no scheme is considered to counteract the effects of robot dynamics, so these “abrupt” movements will remain present, but on a small scale. For all cases, the speed in the engines is below the maximum value established by the manufacturer (113.5 rpm). The times for the

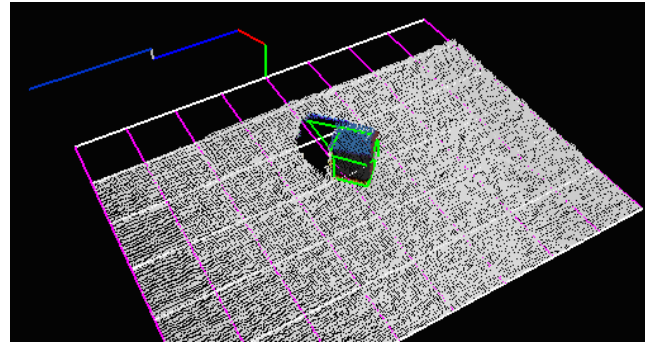


Fig. 8 Error in the correspondence between 2D and 3D data.

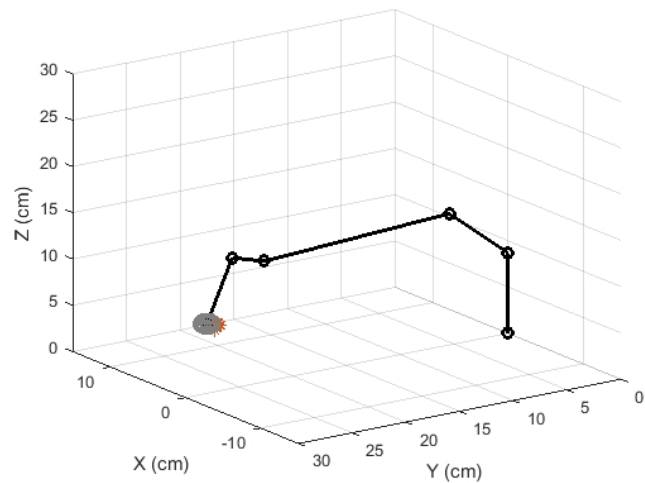


Fig. 9 A robotic arm reached in space.

trajectories of movement of the first three degrees of freedom were 5, 8 and 4s, respectively, regarding accuracy in repeatability, tests were performed to determine how close the end of the robotic arm reached a point in space, without considering the existence of the end effector (clamp) (Fig. 9).

Table 1 Rotations.

Rotation	Image Information		System Information		Recognition Percentage	
	Number of Lines	Parallel Lines Pairs	Number of Lines	Parallel Lines Pairs	Lines	Parallel Lines Pairs
0°	7	3	4	1	42.85%	33.33%
20°	9	6	5	1	66.66%	16.66%
40°	9	6	7	2	66.66%	33.33%
60°	9	6	7	1	66.66%	16.66%
80°	7	3	4	0	42.85%	0.00%
100°	9	6	6	1	66.66%	16.66%
120°	9	6	6	2	66.66%	33.33%
140°	9	6	5	1	55.55%	16.66%
160°	7	3	4	0	57.14%	0.00%

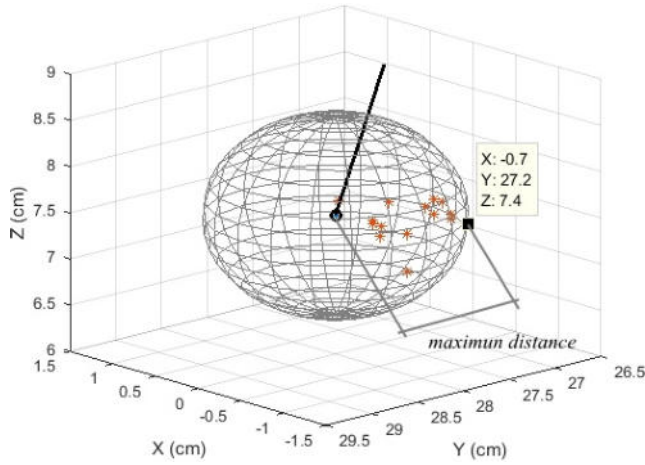


Fig. 10 Representation of the resolution of the robotic arm.

In Fig. 10, the repeatability of the robotic⁴² arm is presented as a sphere that encloses the set of positions to which the arm can return given a target position and certain test conditions, where the maximum distance to the target from a measured point is ± 10.6 mm.

3.5. Expert System with Machine Learning Results on BIoT

The development of the expert system has the one-terabyte database, a 7th generation Intel CORE I7 processor with a GTX 1070 GPU. A precision of 97% was obtained in the semantic search engine. Table 2 shows the comparative results using three algorithms: SHA256 and SCRYPT.

Table 2 shows the dynamic performance of the searches on the IoT platform, where L represents the number of entries, N represents the number of hidden nodes per layer, M represents the size of the

Table 2 Blockchain Algorithms Comparative Performance (m).

Algorithm	Parameters	Training (seconds)	Testing (seconds)
(SHA256)	$L = 843$ $N = 10$ $M = 1$ Terabyte $D = 7$	25	39
(SCRYPT)	$L = 843$ $N = 10$ $M = 1$ Terabyte $D = 7$	17	21

Table 3 Hyperparameter of a Deep Network Range.

	Units per Layer	Layers	Pre-Training rate	Fine Adjustment Rate
Minimum	2	2	0.03	0.3
Maximum	7	4	0.2	0.5

Table 4 Comparative Table for ELM, MLP and DL.

	ELM	MLP	DL	
COST ($\times 10^{-3}$)	13	21	6.5	
DL	Binary (0, 1)	Continuous (0, ∞)	Continuous (0, 1)	Continuous (-6, 6)
COST ($\times 10^{-3}$)	7	21	5.5	7.3

database and; D the number of depth layers (DL dimension).

The parameters used in the DL net for this study are shown in Table 3.

The deep belief network helps to minimize the dimensionality effect problem in the deep architecture models. It is observed that using only two identification layers, we can have a minimal testing error, nevertheless, on the medium region of the surface, it is noticed that when increasing the number of layers and units, we can get to a new magnitude local minimal from the studied error (ideal deep dimension).

Table 4 shows a comparative performance between three different neural network structures: extreme learning machine (ELM), Multilayer perceptron (MLP) and DL.

4. DISCUSSION

By using the Canny filter and the Hough transform, it was observed that these methods can be more efficient when using images in which larger objects exist, however, the limitations of the arm did not allow the use of larger objects.

In the post-processing proposal, the maximum angle between vectors (5°) allows the adequate identification of parallel lines. The definition of a reference point allowed relating the position of the object in space with that of the robot, through the inverse kinematics responsible for generating the movement specification of the robot. As a result of identifying two pairs of parallel lines (perpendicular to each other) on the same face of the objects, the choice

of any of the pairs will allow the movement of the object, since the reference point is the same for both pairs of lines.

Regarding the experimental robotic arm used, it should be noted that when performing the clamping tests, it was observed that the weight of the objects that can be moved is 140 grams, which is less than the specification of 1 kg of load for the robot, this obeys mainly to how the objects are taken. On the implementation of a speed profile,^{43–45} this favored the transfer of objects, allowing to reach an objective position without falling during the journey, however, there are still minor abrupt movements due to the lack of a scheme to counteract the dynamic effects of movement itself.^{46–51}

It should be noted that the variations (measured as absolute mean error) presented in the calculated reference points concerning the real values, is a product of both the location of the Kinect depth sensor and the implicit coordinate transformation, as well as of the processing operations and interpretation of the image.^{52–54} However, despite these variations and the limitations of the robotic arm itself, the system allowed the robotic arm to be correctly located to take and move the object.

5. CONCLUSIONS

In this paper, we present the development of a capable system of identifying parallel edges in simple objects (rectangular prisms), to manipulate them using an experimental robotic arm. However, when considering the 2D image as the primary source of information, the system is susceptible to changes in luminosity in the environment, which impacts the 33.33% recognition of parallel lines obtained.

According to Table 4, DL is really the best choice comparing to ELM and MLP with the best cost.

Since this is a preliminary work, several future works are proposed with assistance of the knowledge society concepts,^{55,56} such that they can help us to better understand the impact and usage of this technology for the society, under the principle that a big advance in technology makes society transformation though a knowledge spread easily, a good approach of an enhancement on this technology could be, for example, the use of another Kinect sensor that is located in a position above the robotic arm, which would facilitate the recognition of the closest faces or objects to the robotic arm and would grant greater versatility to manipulation.^{57–60}

REFERENCES

1. S. Pradip, C. Mu-Yen and P. Jong, A software-defined fog node based distributed blockchain cloud architecture for IoT, *IEEE Access* **6**(99) (2017) 115–124.
2. J. Sun *et al.*, Blockchain-based sharing services: What blockchain technology can contribute to smart cities, *Financ. Innov.* **2**(26) (2016) 1–9.
3. J. L. Zhao, Overview of business innovation and research opportunities in blockchain and introduction to the special issue, *Financ. Innov.* **3**(9) (2017) 1–7.
4. T. Aste, P. Tasca and T. D. Matteo, Blockchain technologies: The foreseeable impact on society and industry, *Computer* **50**(9) (2017) 18–28.
5. M. E. Peck and D. Wagman, Energy trading for fun and profit buy your neighbor's rooftop solar power or sell your own-it'll all be on a blockchain, *IEEE Spectr.* **54**(10) (2017) 56–61.
6. L. Cheng and Z. Liang-Jie, A blockchain based new secure multi-layer network model for internet of things, in *IEEE International Congress on Internet of Things (ICIOT)*, Honolulu, USA (IEEE, 2017), pp. 33–41.
7. J. Sidhu, Syscoin: A Peer-to-peer electronic cash system with blockchain-based services for e-business, in *26th Int. Conf. Computer Communication and Networks (ICCCN)*, Vancouver, Canada (IEEE, 2017), pp. 1–6.
8. H. Kim and M. Laskowski, A perspective on blockchain smart contracts: Reducing uncertainty and complexity in value exchange, in *26th Int. Conf. Computer Communication and Networks (ICCCN)*, Vancouver, Canada (IEEE, 2017), pp. 1–6.
9. Blockone, EOS.IO Technical White Paper v2 (2018), <https://github.com/EOSIO/Documentation/blob/master/TechnicalWhitePaper.md>.
10. Blockone, Developers, <https://developers.eos.io/eosio-home/docs>.
11. M. Samaniego and R. Deters, Internet of smart things — IoST: Using blockchain and CLIPS to make things autonomous, in *IEEE Int. Conf. Cognitive Computing (ICCC)* (IEEE, 2017), pp. 9–16.
12. F. K. Flores, Internet of things: Managing wireless sensor network with rest API for smart homes, in *Theory and Practice of Computation*, Manila, 2016, pp. 132–142.
13. R. Carreño *et al.*, An IoT expert system shell in block-chain technology with elm as inference engine, *Int. J. Inf. Tech. Decis. Mak.* **18**(1) (2019) 87–104.
14. A. D. Alonso and E. A. Jara, *Visión Por Computadora: Identificación, Clasificación y Seguimiento de Objetos* (FPUNE Scientific, 2016), pp. 17–28.
15. B. Rasolzadeh, M. Björkman, K. Hübner and D. Kragic, An active vision system for detecting,

- fixating and manipulating objects in real world, *Int. J. Robot. Res.* **29**(2) (2009) 133–154.
16. C. K. Wong, P. P. Lim, R. Clist and L. R. ShuHe, Vision strategies for robotic manipulation of natural objects, in *Australasian Conf. Robotics and Automation (ACRA)*, Sydney, Australia (2009).
 17. M. S. Hernández, *Determinación y Localización Espacial de Objetos Geométricos Simples Para la Manipulación Por un Robot Móvil Autónomo*, Tesis de Maestría Universidad Veracruzana, Veracruz, Mexico (2011).
 18. P. I. Corke, *Robotics, vision and control fundamental algorithms in MATLAB* (Springer-Verlag, Australia, 2017).
 19. D. Kragic and H. I. Christensen, Survey on visual servoing for manipulation, *Comput. Vis. Act. Percept. Lab.* **1** (2002) 1–10.
 20. L. M. Bueno and P. M. Arteaga, Control servovisual de robots manipuladores: Un enfoque hacia la industria, *Épsilon* **19** (2012) 9–31.
 21. L. Bodenhagen, A. R. Fugl, A. Jordt, M. Willatzen, Aulkjær, K. Andersen and N. Krüger, An adaptable robot vision system performing manipulation actions with flexible, *IEEE Trans. Autom. Sci. Eng.* **11**(3) (2014) 749–765.
 22. D. Holz, D. Nieuwenhuisen, D. Droschel, J. Stuckler, A. Berner, J. Li and S. Behnke, *Active Recognition and Manipulation for Mobile Robot Bin Picking*, Springer Tracts in Advanced Robotics (Springer, 2014), pp. 133–153.
 23. A. Sanderson and L. Weiss, Image-based visual servo control using relational graph error signals, in *Proc. Int. Conf. Cybernetics and Society*, Cambridge, MA (IEEE SMC, 1980), pp. 1074–1077.
 24. S. Rionero, Lyapunov functionals for the coincidence between the first and the second lyapunov stability methods, *New Trends in Fluid and Solid Models*, 1st edn. (World Scientific, Italy, 2009), pp. 113–121.
 25. Y. Wang, Y. Ewert, R. Vossen and S. Jeschke, Visual servoing system for interactive human-robot object transfer, *J. Autom. Control Eng.* **3**(4) (2015) 277–283.
 26. N. K. Lakshmi, M. Sujana and B. Polaiiah, Automatic detection and distinction of colored objects using color sorting robotic arm for industrial application, *Int. J. Adv. Res. Manage.* **2**(6) (2016) 328–331.
 27. W. Gu *et al.*, Expert system for ice hockey game prediction: Data mining with human judgment, *Int. J. Inf. Technol. Decis. Mak.* **15**(4) (2016) 763–789.
 28. N. J. Pizzi *et al.*, Expert system approach to assessments of bleeding predispositions in tonsillectomy/adenoidectomy patients, *Adv. Artif. Intell.* **27** (1990) 67–83.
 29. P. Agrawal, V. Madaan and V. Kumar, Fuzzy rule-based medical expert system to identify the disorders of eyes, ENT and liver, *Int. J. Adv. Intell. Paradigms* **7** (2015) 352–367, doi:10.1504/IJAIP.2015.073714.
 30. A. H. Dong, D. Shan, Z. Ruan, L. Y. Zhou and F. Zuo, The design and implementation of an intelligent apparel recommend expert system, *Math. Prob. Eng.* **2013** (2013) 1–8, doi:10.1155/2013/343171.
 31. P. Som, R. Chitturi, A. J. G. Babu, Expert systems application in manufacturing, in *Proc. Applications of Artificial Intelligence*, International Society for Optics and Photonics, Vol. 786 (1987), pp. 474–479, doi:10.1117/12.940659.
 32. B. Fu, The Research of Agricultural Expert System based on IOT, in *4th International Conference on Computer, Mechatronics, Control and Electronic Engineering (ICCMCEE 2015)* (Atlantis Press, 2015), doi:10.2991/iccmcee-15.2015.262.
 33. L. Yu *et al.*, Prediction-based multi-objective optimization for oil purchasing and distribution with the NSGA-II algorithm, *Int. J. Inf. Technol. Decis. Mak.* **15**(2) (2016) 423–451.
 34. W. Yu *et al.*, Neural networks for the optimization of crude oil blending, *Int. J. Neural Syst.* **15**(5) (2005) 377–389.
 35. B. Iscimen, H. Atasoy, Y. Kutlu, S. Yildirim and E. Yildirim, Smart robot arm motion using computer vision, *Elektron. Elektrotech.* **21**(6) (2015) 1–7.
 36. H. Wu, T. T. Andersen, N. A. Andersen and R. Ole, Visual servoing for object manipulation: A case study in slaughterhouse, in *Proc. Int. Conf. Robotics and Automation IEE*, Phuket, 2016.
 37. J. N. Pires, Robot manipulators and control systems, in *Industrial Robots Programming: Building Applications for the Factories of the Future* (Springer, Boston, MA, 2007).
 38. B. Siciliano, and O. K. Khatib, *Handbook of Robotics* (Springer, 2016).
 39. Anh Tuan Vo & Hee-Jun Kang, An adaptive neural non-singular fast-terminal sliding-mode control for industrial robotic manipulators, *Appl. Sci.* **8**(12) (2018) 2562.
 40. L. Celentano, A unified approach to design robust controllers for nonlinear uncertain engineering systems, *Appl. Sci.* **8**(11) (2018) 2236.
 41. L. Zhang, J. S. Dhupia, M. Wu and H. Huang, A robotic drilling end-effector and its sliding mode control for the normal adjustment, *Appl. Sci.* **8**(10) (2018) 1892.
 42. M. M. Rami Alazrai and I. D. Mohammad, Fall detection for elderly from partially observed depth-map video sequences based on view-invariant human activity representation, *Appl. Sci.* **7**(4) (2017) 316.
 43. J. Patiño *et al.*, Seismic activity seen through evolution of the Hurst exponent model in 3D, *Fractals* **24**(4) (2016) 1–4.

44. M. Choda, Around Shannon's interpretation for entropy preserving stochastic averages, *Int. J. Math.* **25**(10) (2014) 1–4.
45. V. S. Pugachev, *Theory and Mathematical Statistics for Probability Engineers* (Pergamon Press, Oxford, 1984).
46. R. Carreño et al., A nonlinear acoustic transducer model with variable structure control, *Fractals* **25**(2) (2017) 1–6.
47. W. Yu et al., Modeling of gasoline blending via discrete time neural networks, *Neural Netw. Proc.* **6** (2004).
48. W. Yu and X. Li, Automated nonlinear system modeling with multiple fuzzy neural networks and kernel smoothing, *Int. J. Neural Syst.* **20**(5) (2010) 429–435.
49. S. Lu et al., Nonlinear autoregressive and nonlinear autoregressive moving average model parameter estimation by minimizing hypersurface distance, *IEEE Trans. Signal Process.* **51**(12) (2003) 3020–3026.
50. R. Carreño et al., Comparative analysis on nonlinear models for ron gasoline blending using neural networks, *Fractals* **25**(6) (2017) 1–8.
51. D. Pacheco et al., Nonlinear fm index application for alignment of short dna sequences using re-parametrization of algorithms, *Fractals* **26**(3) (2018) 11.
52. L. Sheng and J. Hwan, A new algorithm for linear and nonlinear ARMA model parameter estimation using affine geometry, *IEEE Trans. Biomed. Eng.* **48**(10) (2001) 1116–1124.
53. J. J. Carrasco, ELM regularized method for classification problems, *Int. J. Artif. Intell. Tools* **25**(1) (2016) 1–12.
54. G. B. Huang, what are extreme learning machines? Filling the gap between Frank Rosenblatt's dream and John von Neumann's puzzle, *Cogn. Comput.* **7**(3) (2015) 263–278.
55. P. Weingart, The moment of truth for science: The consequences of the 'knowledge society' for society and science, *EMBO Rep.* **3**(8) (2002) 703–706.
56. Tobón et al., Sociedad del conocimiento: Estudio documental desde una perspectiva humanista y compleja, *Paradigma* **362** (2015) 7–36
57. Y. li, Extreme learning machine for determining signed efficiency measure from data, *Int. J. Uncertainty, Fuzziness Knowledge-Based Syst.* **21**(2) (2013) 131–142.
58. H. T. Huynh et al., An improvement of extreme learning machine for compact single-hidden-layer feedforward neural networks, *Int. J. Neural Syst.* **18**(5) (2008) 433–441.
59. Wei Gu et al., Expert system for ice hockey game prediction: data mining with human judgment, *Int. J. Inf. Tech. Decis. Mak.* **15**(4) (2016) 763–789.
60. C. A Magni et al., An alternative approach to firms' evaluation: Expert systems and fuzzy logic, *Int. J. Inf. Technol. Decis. Mak.* **5**(1) (2016) 195–225.